Structural Characterization and Dynamic Water Adsorption of Electrospun Polyamide6/ Montmorillonite Nanofibers

Qi Li, Qufu Wei, Ning Wu, Yibing Cai, Weidong Gao

Key Laboratory of Eco-textiles, Ministry of Education, Jiangnan University, Wuxi 214122, People's Republic of China

Received 5 June 2007; accepted 15 October 2007
DOI 10.1002/app.27529
Published online 3 December 2007 in Wiley InterScience (www.interscience.wiley.com).

ABSTRACT: A facile compounding process, which combined nanocomposite process with electrospinning for preparing novel polyamide6/organic modified montmorillonite (PA6/O-MMT) composite nanofibers, is reported. In this compounding process, the O-MMT slurry was blended into the formic acid solution of PA6 at moderate temperatures, where the nanosized O-MMT particles were first dispersed in *N*,*N*-dimethyl formamide solvent homogeneously via ultrasonic mixing. Subsequently the solution via electrospinning formed nanofibers, which were collected onto aluminum foil. The O-MMT platelets were detected to be exfoliated at nanosize level and dispersed homogeneously along the axis of the nanofibers using an electron transmission microscope. Scanning electron microscope and atomic force microscope were used to analysis the size and surface morphology of polyamide6/O-MMT composite nanofibers. The addition of O-MMT reduced the surface tension and viscosity of the solution, leading to the decrease in the diameter of nanofiber and the formation of rough and ridge-shape trails on the nanofiber surface. The behavior of the dynamic water adsorption of composite nanofibers was also investigated and discussed in this article. © 2007 Wiley Periodicals, Inc. J Appl Polym Sci 107: 3535–3540, 2008

Key words: electrospinning; montmorillonite; composite; nanofiber; water adsorption

INTRODUCTION

The polymer/montmorillonite silicate nanocomposite (PMSN) materials have attracted great attention to researchers in recent years. It has been found that PMSN materials indicated increased modulus, strength, and improved thermal and barrier properties.[1–8] The significant improvement in the properties of PMSN materials can be achieved with the silicate content lower than 5% when the silicate layers are homogeneously exfoliated in the polymer matrix due to the nanometer size and high surface area of silicate layers.[1] The most investigations have focused on the molded materials[4–8] with few researches reporting on the formation and properties of PMSN fibers by electrospinning.[1–3]

Polyamide6 (PA6) has been studied for many years due to its expanded applications. The PA6/Na-montmorillonite nanocomposites, loaded with only 1.6 wt % clay silicate layers, exhibited high strength, high modulus, high heat distortion temperature, and low gas permeability compared to neat polyamide6.[4] In addition, it was reported that the mechanical properties of the electrospun polyamide6/Na-montmorillonite fibrous mats were significantly improved, compared to the neat polyamide6 fibrous mats which was well studied using an atomic force microscope (AFM).[1]

However, most of the compounding processes have concentrated on the melting-extrude techniques for making the PMSN slices. Hasegawa et al.[4] reported another compounding process that was using Na-montmorillonite water slurry for preparing novel nylon 6/Na-montmorillonite nanocomposites where the Na-montmorillonite slurry was blended with melting nylon 6 using an extruder, followed by removing the water. In this research, a facile and economy composite technique was provided. It was that, order to buildup the hydrophobicity surface structure and initially exfoliate to thinner layers, the montmorillonite powder modified with a quaternary ammonium ion at the melting state (organic montmorillonite, abbreviated as O-MMT), was dispersed in the *N*,*N*-dimethyl formamide and then compounded with polyamide6 which was dissolved in formic acid. The composite solution was spun to form a fibrous mat using the electrospinning technique. The formation of the fibrous mats was investigated by scanning electron microscopy (SEM),

Correspondence to: Q. Wei (qfwei@jiangnan.edu.cn).
Contract grant sponsor: Specialized Research Fund for the Doctoral Program of Higher Education; contract grant number: 20060295005.
Contract grant sponsor: Program for New Century Excellent Talents in University; contract grant number: NCET-06-0485.

TABLE I
Sample Specifications

Sample	A	B	C
Polyamide6 (wt %)	18	18	18
O-MMT (wt %)	0	1	2

and the surface morphology of a single nanofiber was examined using AFM. The dynamic water adsorbtion of the nonwoven fabrics made of nanofibers was also investigated and discussed.

EXPERIMENTAL

Materials

The organically modified montmorillonite (O-MMT) was purchased from Zhejiang Fenghong Clay Chemicals Co. (China). The average thickness of the particle was less than 25 nm, and the ratio of diameter to thickness was about 200. Polyamide6 (characteristic viscosity was 2.8), 99.5% *N*,*N*-dimethyl formamide (DMF), and 88% formic acid were all used as received.

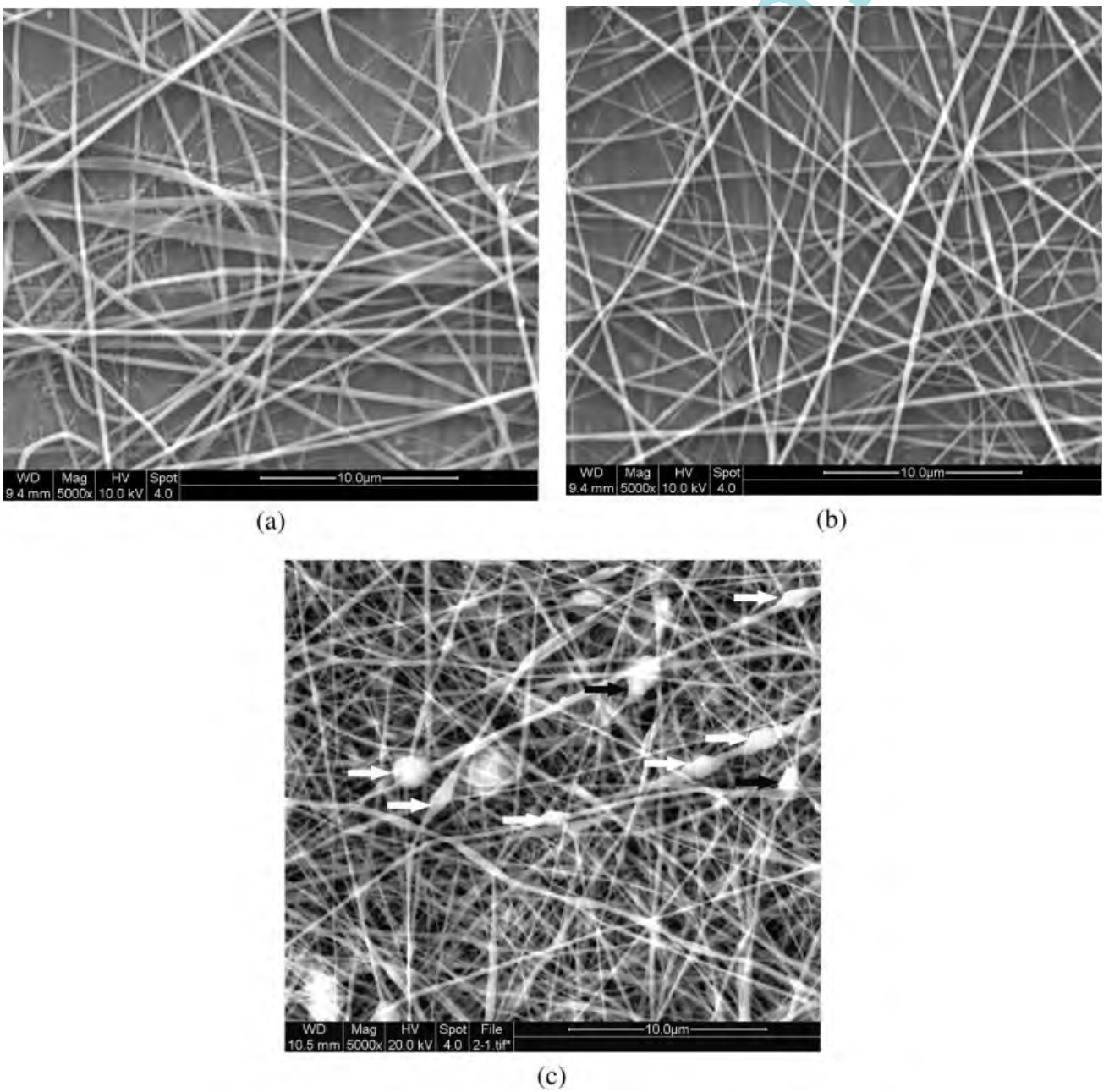

Figure 1 SEM images of electrospun nanofibers (a) Sample A, (b) Sample B, (c) Sample C.

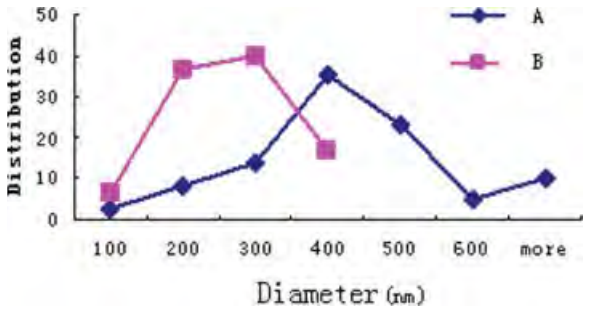

Figure 2 The distribution of nanofiber diameters. [Color figure can be viewed in the online issue, which is available at www.interscience.wiley.com.]

Preparation of composite nanofibers

The clay slurry was prepared by dispersing O-MMT (4 g) dry power into DMF (48.52 mL) solvent using magnetic stirring for 20 min until the powder uniformly dispersed in the DMF solvent. Polyamide6 (18 wt %) dissolved in formic acid was also prepared. The prepared clay slurry was then put into the polyamide6 solution, which was mixed in an ultrasonic bath for another 40 min. The sample specifications are listed in Table I.

The electrospinning apparatus consisted of a syringe, a needle, and a high-voltage power in which a positive voltage (16 kV) was applied to the polymer solution through the needle attached to the syringe. The solution jet was formed by electrical force, when the electrical potential increased to 16 kV. The nanofibers in a nonwoven form were collected on an aluminum foil. The ejection rate of the solution was 0.2 mL/h, and the distance between the tip and the collector was 12 cm.

Surface tension and viscosity

The surface tensions and viscosities of the prepared solutions for the electrospinning were measured. Surface tension tests were performed by CDCA-100F, made by the Camtel, UK. All the tests were done at 20 ± 2 °C. The viscosity tests were carried out by using a rotary viscometer NDJ-79 and all the tests were made at 20 ± 2 °C.

Structural characterization of nanofibers

SEM Quanta 200 was used to examine the structures of the nanofiber web. The samples were coated with a thin layer of gold by sputtering before the SEM imaging. The diameters of the nanofibers were measured by ImageJ software based on the SEM images and 100 nanofibers were randomly selected from each sample. In addition, the AFM was used to further observe the surface structures of the nanofibers. The AFM used in this work was a Benyuan CSPM 4000. Scanning was carried out in tapping mode. All images were obtained at ambient conditions.

The dispersibility of the O-MMT platelets in the nanofibers was examined using a transmission electrical microscope (TEM). The TEM used was Hitachi H-7000. The nanofibers were collected on a TEM grid for the TEM observation.

Measurement of dynamic water adsorption

Dynamic water adsorption tests were performed on a Camtel CDCA-100F dynamic adsorption apparatus (made by the Camtel Ltd, UK). The size of the nanofiber samples was 1 cm × 6 cm. The tests were carried out at a temperature of 20 ± 1°C. When the specimen was immersed into the water, the water adsorption was detected and recorded. The dynamic water adsorption was plotted as a function of time.[9]

RESULTS AND DISCUSSION

Fibrous structures of the nanofibers

The electrospun nanofibers of the neat PA6 and PA6/O-MMT solutions show different fiber diameters and distributions detected by the SEM observation. The electrospun nanofibers of the neat PA6 and PA6/O-MMT solutions collected on the aluminum foil form fibrous webs as illustrated in Figure 1. The nanofibers are randomly distributed to form the fibrous web. It is observed that the nanofibers electrospun from neat PA6 and PA6/O-MMT solutions both show variable fiber diameters. The SEM images reveal that the nanofibers spun from the neat polyamide6 show a wider range of fiber diameter distribution as displayed in Figure 2. Compared to the neat PA6 nanofibers, however, the diameters of the composite nanofibers containing 1% O-MMT show a relatively narrower distribution, as indicated in Figure 2. It is also observed from Figure 2 that the diameters of the neat polyamide6 nanofibers become finer than those of the composite nanofibers containing 1% O-MMT. It is well known that the production of nanofibers by the electrospinning process is affected by the combination of the electrostatic forces and the viscoelastic behavior of the polymer

TABLE II
Surface Tension and Viscosity

Sample	A	B	C
Surface tension (mN/m)	42.5 ± 0.5	40.3 ± 0.5	38.6 ± 0.5
Viscosity (Pa s)	1.563 ± 0.05	1.193 ± 0.05	0.707 ± 0.05

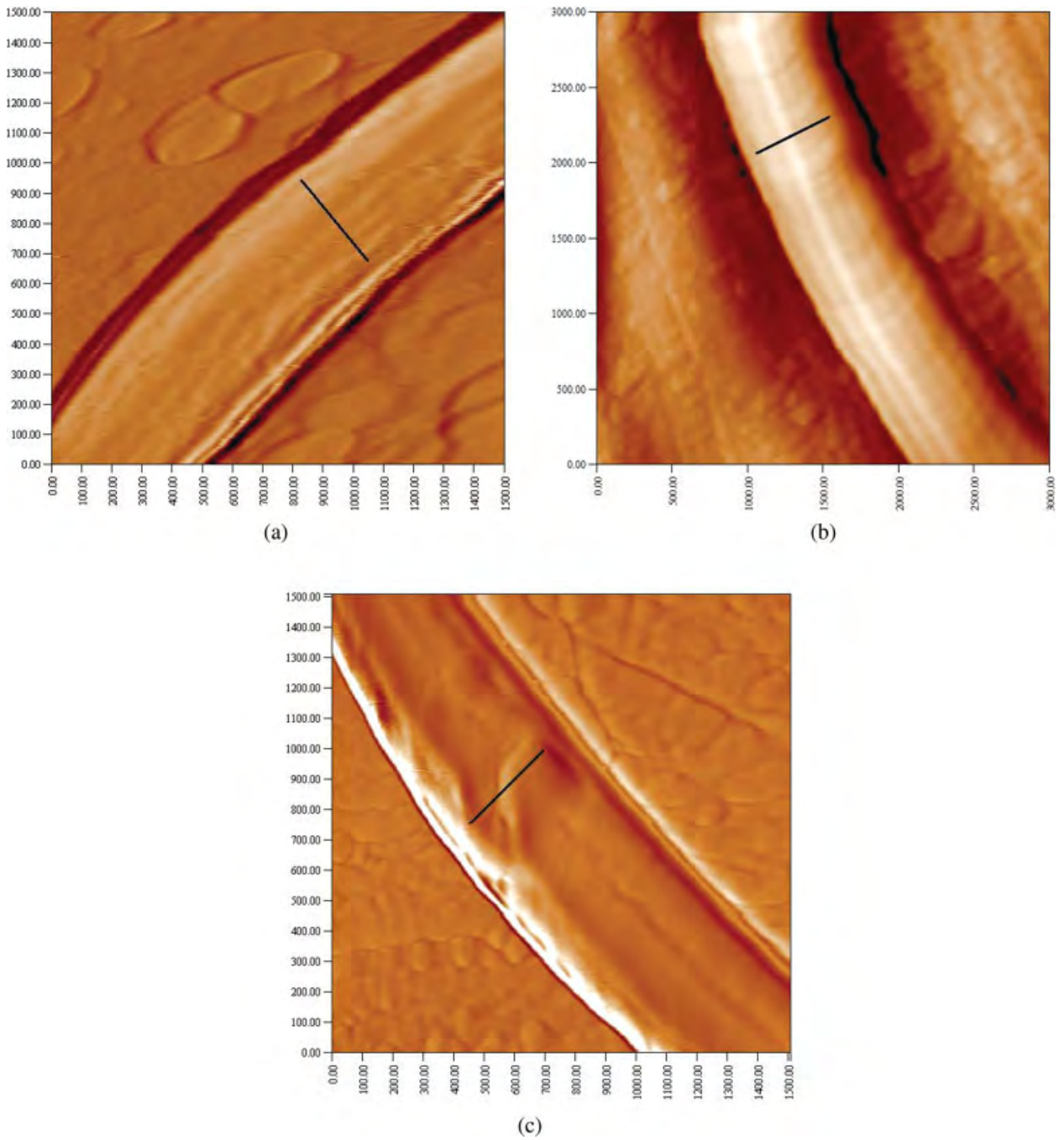

Figure 3 AFM images of electrospun nanofibers (a) Sample A, (b) Sample B, (c) Sample C. [Color figure can be viewed in the online issue, which is available at www.interscience.wiley.com.]

solution. The viscoelastic behavior of the polymer solution plays the most importance role in this study since the electrostatic forces applied are fixed. The lower surface tension and viscosity of the Sample B, as indicated in Table II, contribute to the formation of the narrowly distributed finer nanofibers. In the electrospinning process, the ejected drop will overcome the surface tension and be accelerated in the high electric field, and then deposited on the aluminum foil when the electrical force is far more the surface tension of the solution. The decrease in the viscosity also facilitates the stretch of the jet in the electrical field, leading to the formation of finer fibers.

The SEM image in Figure 1(c) clearly reveals the formation of beaded structures of the nanofibers when the O-MMT content is increased to 2%. Some beaded fibers are formed by the aggregation of the O-MMT, as shown by black arrows in Figure 1(c). The most beaded fibers [marked by white arrows in

Fig. 1(c)], however, are formed due to the lowest surface tension and viscosity of the Sample C, as shown in Table II. In electrospinning process, the coiled macromolecules in the polymer solution are transformed by a stretched flow of the jet into nanofibers. The beaded nanofibers are formed if the surface tension and viscosity are insufficient for stabilizing the jet.[10] This is also the reason why our results are different from those presented in Ref. 2.

Surface morphology of the nanofibers

The SEM images reveal the fibrous structures of the nanofibers. The AFM images with a much higher resolution further reveal the surface morphology of the nanofibers as presented in Figure 3. The neat PA6 nanofibers show a relatively smooth surface, as indicated in Figure 3(a), but the composite nanofibers containing 1% O-MMT show ravine-shape structures both in transverse and axis directions, as presented in Figure 3(b). Nevertheless, the AFM image of the nanofiber loaded with 2 wt % O-MMT in Figure 3(c) seems to be much more coarse, have some big long ravines and a relative wide height movement, compared to the neat PA6 and the composite nanofiber containing 1 wt % O-MMT.

It is obtained by the AFM image software that the roughness average (RA) of Sample A is 5.70 nm, Sample B is 12.64 nm, and Sample C is 21.13. The results of the roughness are obtained from line-section on the nanofiber surface, as marked by the black lines in Figure 3. The structure transformation of the nanofiber surface is mainly affected by the solvent vapor and viscoelastic behavior of the polymer solution. It is believed that the lower viscosity and surface tension of the polymer solution directly results in the rapider or excessively solvent volatilization, leading to the formation of smaller fiber diameters and the rougher surface of the nanofibers.

O-MMT in nanofibers

The TEM observation reveals the formation of the composite nanofibers and the distribution of the O-MMT nanoparticles in the nanofiber matrix. The TEM image in Figure 4 indicates the nanosize O-MMT clayers in the PA6 nanofibers electrospun from the solution containing 2 wt % O-MMT. It can be clearly observed that each silicate platelet forms a dark line in the nanofiber. The size of the dark line is about 1–3 nm in width and 15–20 nm in length, indicating the good dispersion and exfoliation of O-MMT layers in the nanofibers. The TEM images also clearly reveal that the clayers are almost aligned along the nanofiber axis, and some would bend during the electrospinning process, as shown in the third images in Figure 4.

The solvent used in this study was formic acid, which can form hydrogen bonds and hydroxyl groups on the surface of O-MMT platelets. Electrostatic interaction may also occur between the charged O-MMT surfaces and formic acid molecules. However, the hydrogen bonding and electrostatic interactions between O-MMT layers and the solvent do not cause phase separation between PA6 molecules and O-MMT layers in the solution or reagglomeration of the O-MMT. The exfoliation of O-MMT is attributed to the hydrogen bonding between

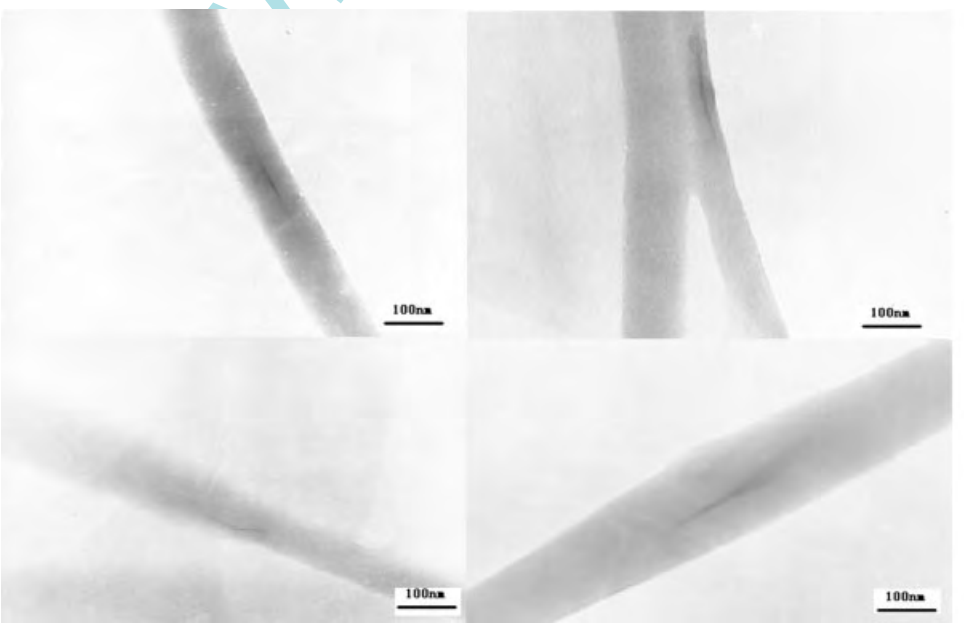

Figure 4 TEM images of electrospun nanofibers.

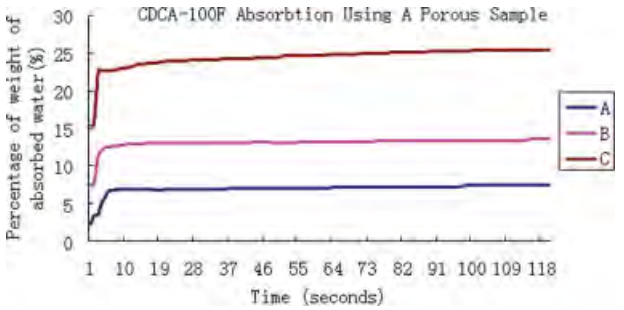

Figure 5 Water adsorption of fibrous mats. [Color figure can be viewed in the online issue, which is available at www.interscience.wiley.com.]

DMF and O-MMT, effectively leading to phase separation between O-MMT and PA6.[1]

Water adsorption analysis

The testing results of dynamic water adsorption illuminate the water adsorption behavior of the electrospun nonwoven nanofibers, as shown in Figure 5. All the samples tested show a good water adsorption with a very sharp initial adsorption rate,[9] when the samples are immersed into the water. It can be seen that the samples appear to show better water absorption as the content of the O-MMT is increased. The water adsorption curves in Figure 5 reveal that the neat PA6 nanofibers show the water adsorption from the initial 2.02% up to a maximum 7.40%. The water adsorption of the Sample B reaches 13.57% from 7.43% and the Sample C from 15.41% to about 25.45%. The results clearly reveal that the water adsorption is improved with the addition of O-MMT.

The structures of the nanofibers have a great influence on the behavior of water adsorption. Compared to the neat PA6 nanofibers, the composite nanofibers have much more coarseness and ridge-shape surface morphology structure (as shown in the AFM images), which will increase the contact area between the nanofibers and water molecules and consequently improve the water adsorption. On the other hand, the smaller fiber diameters will directly contribute to the capillary effect of the nanofibers, leading to the better water adsorption.

CONCLUSION

This study has explored the structural characteristic, surface morphology, and water adsorption of the electrospun PA6/O-MMT composite nanofibers. The addition of O-MMT in PA6 matrix decreased the surface tension and viscosity of the composite solution, leading to the decrease in nanofiber diameters and the formation of the ridge-shape structures on the nanofiber surface. The O-MMT clays were detected to exfoliate into nanosize layers and align along the axis of the composite nanofibers. The CDCA has detected that the dynamic water adsorption was improved in PA6/O-MMT nanofiber mats compared with neat PA6 nanofiber mats. It is concluded that the structures of the fibrous mats, the surface morphology, and the inner structures affected by the introduction of O-MMT are the main reason for the improvement in the water adsorption.

References

1. Li, L.; Bellan, L. M.; Craighead, H. G. Polymer 2006, 47, 6208.
2. Fong, H.; Liu, W. D.; Wang, C. S.; Vaia, R. A. Polymer 2002, 43, 775.
3. Wang, M.; Hsieh, A. J.; Rutledge, G. C. Polymer 2005, 46, 3407.
4. Hasegawa, N.; Okamoto, H.; Kato, M.; Norio Sata, A. Polymer 2003, 44, 2933.
5. Chavarria, F.; Paul, D. R. Polymer 2004, 45, 8501.
6. Lee, Y. H.; Lee, J. H.; An, I. G.; Kim, C.; Lee, D. S.; Lee, Y. K.; Nam J. D. Biomaterials 2005, 26, 3165.
7. Rodlert, M.; Plummer, C.; Garamszegi, L.; Leterrier, Y.; Grunbauer, H.; Manson, J. Polymer 2004, 45, 949.
8. Chattopadhyay, D. K.; Mishra, A. K.; Sreedhar, B.; Raju, K. V. S. N. Polym Degrad Stab 2006, 91, 1837.
9. Wei, Q. F.; Li, Q.; Wang, X. Q.; Huang, F. L. Polym Test 2006, 25, 717.
10. Jeun, J. P.; Kim, Y. H.; Lim, Y. M.; Choi, J. H.; Jung, C. H.; Kang, P. H.; Nho, Y. C. J Ind Eng Chem 2007, 13, 592.